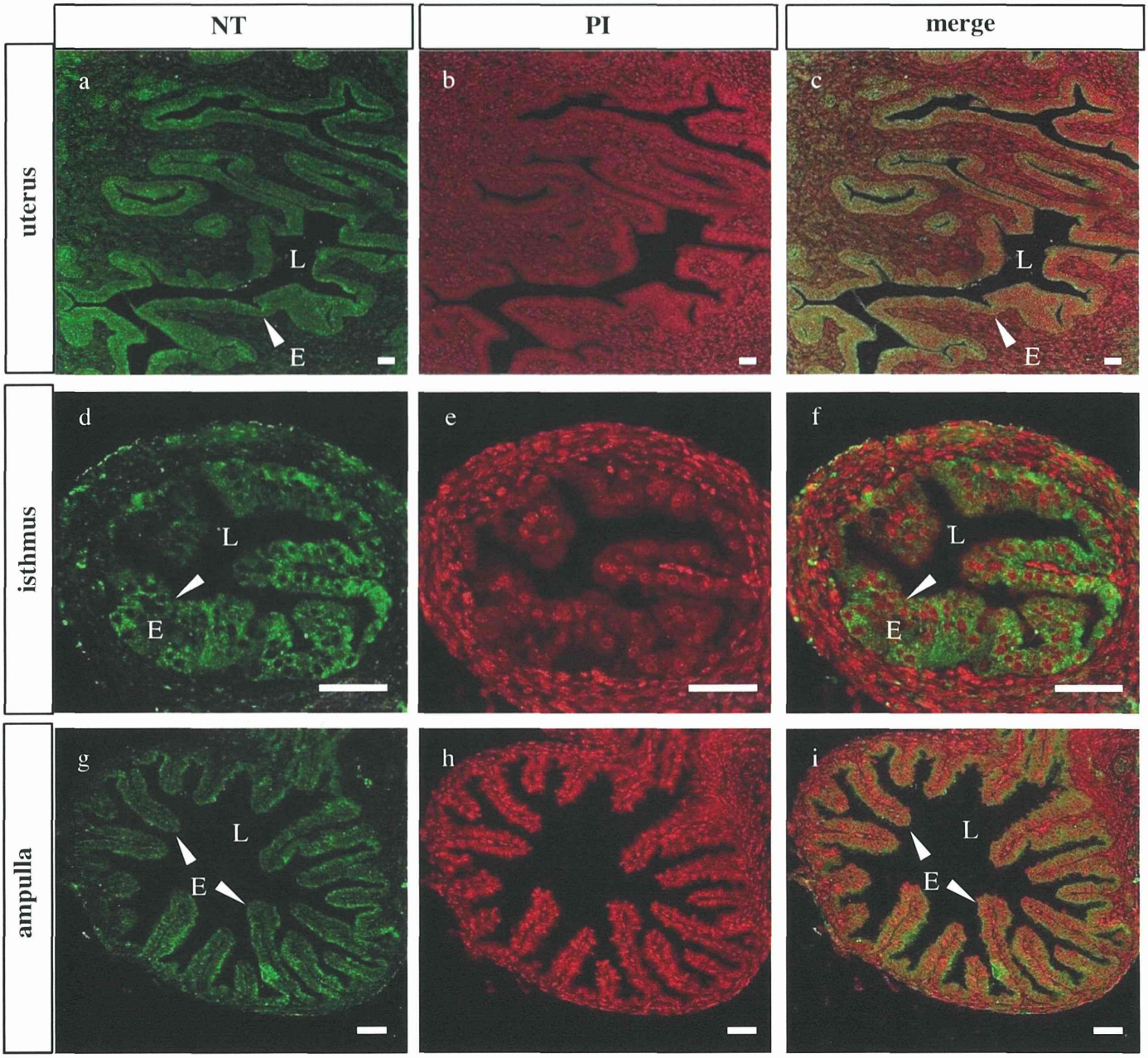

FIG. 6. Immunofluorescence detection of NT in mouse uterus and oviduct. Tissues were collected from immature mice, treated with eCG for 48 h following hCG for 14 h. Fixation was performed in Bouin fixing solution. The samples embedded in paraffin were cut to 5 μm. The uterus (**a–c**), oviduct isthmus (**d–f**), and ampulla (**g–i**) were stained. L = lumen; E = epithelium. Arrowheads indicate immunoreactivity against NT. Green = NT; red = nuclear stain. Bars = 50 μm.

the crucial triggers of oocyte maturation. MAPK activation is induced by phosphorylation with MAPK kinase (MEK) [46]. Because both FSH- and EGF-induced oocyte maturation are mediated by MAPK activation [44, 47], we hypothesized that MAPK also triggers NT upregulation in cumulus cells. Thus, we examined the effects of the MEK inhibitor U0126 on FSH- and EGF-regulated NT mRNA upregulation (Fig. 8). U0126 is a selective inhibitor of MEK-1 and MEK-2. U0126 non-competitively inhibits the catalytic property of MEK and prevents ERK phosphorylation [48]. In the present study, we used U0126 at 1, 5, and 10 μM, and found that both FSH- and EGF-induced upregulation of NT were inhibited, demonstrating that MAPK regulates NT secretion in cumulus cells.

Taken together, our results demonstrate for the first time that NT is secreted from the female reproductive system and enhances sperm capacitation and the acrosome reaction via sperm-expressed functional receptors, NTR1 and presumably NTR2. Moreover, NT is also released from cumulus cells and amplifies gonadotropin stimulation via MAPK activation. This means that NT-NTR interaction is specifically activated and functions at the time of fertilization.

ACKNOWLEDGMENT

The authors thank Dr. Natsuko Kawano for her invaluable advice in sperm experiments and Keita Kosaka, Dr. Masafumi Hidaka, Dr. Hiroshi Yoneyama, Dr. Kouichi Watanabe, Dr. Tomonori Nochi, and Dr. Hisashi Aso for their technical assistance in the preabsorption test.

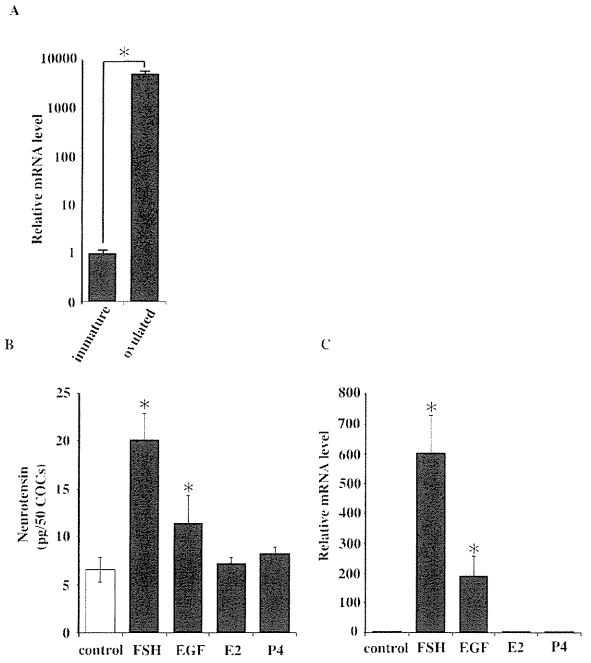

FIG. 7. The changes in NT mRNA levels in cumulus cells primed with eCG and hCG. Cumulus cells were collected from immature mice or from mice superovulated with eCG plus hCG for 14 h. Note that the mRNA level in superovulated cumulus cells was increased (**A**). Data were analyzed by Student *t*-test ($^*P < 0.05$; n = 3). Data are shown as the mean ± SD. The effect of reproductive hormones on NT production by cumulus cells in vitro (**B**). NT concentration at 24 h culture in the presence of FSH (0.1 IU/ml), EGF (50 ng/ml), E2 (100 nM), and P4 (100 nM) was determined by EIA (**C**). E2 and P4 were dissolved in 0.1% DMSO, and 0.1% DMSO was used as a solvent control. Fifty COCs were cultured in each experiment, and NT concentration was determined in the culture medium. The mRNA expression level after 14 h of culture was determined by quantitative RT-PCR. Data were analyzed by one-way ANOVA followed by the Bonferroni-Dunn test, and bars with different letters are significantly different ($^*P < 0.05$; n = 3). Data are shown as the mean ± SD.

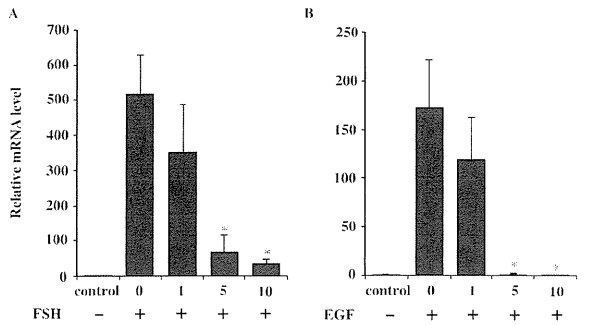

FIG. 8. Effects of MEK inhibitor on NT mRNA expression. The effect of MEK inhibition on NT mRNA expression was determined in in vitro COCs cultured for 14 h in the presence of FSH (0.1 IU/ml), FSH+MEK inhibitor U0126, EGF (50 ng/ml) (**A**), or EGF+U0126 (**B**). U0126 was dissolved in 0.1% DMSO; 0.1% DMSO was used as a solvent control. NT mRNA level was determined by quantitative RT-PCR (n = 3). Data between treatment groups with U0126 at 0 and 1, 5, or 10 μM were analyzed using Student *t*-test. Data are shown as the mean ± SD.

REFERENCES

1. Yanagimachi R, Chang MC. Fertilization of hamster eggs in vitro. Nature 1963; 200:281–282.
2. Visconti PE, Moore GD, Bailey JL, Leclerc P, Connors SA, Pan D, Olds-Clarke P, Kopf GS. Capacitation of mouse spermatozoa. II. Protein tyrosine phosphorylation and capacitation are regulated by a cAMP-dependent pathway. Development 1995; 121:1139–1150.
3. Visconti PE, Ning X, Fornes MW, Alvarez JG, Stein P, Connors SA, Kopf GS. Cholesterol efflux-mediated signal transduction in mammalian sperm: cholesterol release signals an increase in protein tyrosine phosphorylation during mouse sperm capacitation. Dev Biol 1999; 214:429–443.
4. Puente MA, Tartaglione CM, Ritta MN. Bull sperm acrosome reaction induced by gamma-aminobutyric acid (GABA) is mediated by GABAergic receptors type A. Anim Reprod Sci 2011; 127:31–37.
5. Ramírez AR, Castro MA, Angulo C, Ramió L, Rivera MM, Torres M, Rigau T, Rodriguez-Gil JE, Concha II. The presence and function of dopamine type 2 receptors in boar sperm: a possible role for dopamine in viability, capacitation, and modulation of sperm motility. Biol Reprod 2009; 80:753–761.
6. Meizel S, Turner KO. Serotonin or its agonist 5-methoxytryptamine can stimulate hamster sperm acrosome reactions in a more direct manner than catecholamines. J Exp Zool 1983; 226:171–174.
7. Carraway R, Leeman SE. The isolation of a new hypotensive peptide, neurotensin, from bovine hypothalami. J Biol Chem 1973; 248: 6854–6861.
8. Thibault D, Albert PR, Pineyro G, Trudeau LE. Neurotensin triggers dopamine D2 receptor desensitization through a protein kinase C and beta-arrestin1-dependent mechanism. J Biol Chem 2011; 286:9174–9184.
9. Binder EB, Kinkead B, Owens MJ, Nemeroff CB. Neurotensin and dopamine interactions. Pharmacol Rev 2001; 53:453–486.
10. Carraway R, Leeman SE. Characterization of radioimmunoassayable neurotensin in the rat. Its differential distribution in the central nervous system, small intestine, and stomach. J Biol Chem 1976; 251:7045–7052.
11. Zhao D, Pothoulakis C. Effects of NT on gastrointestinal motility and secretion, and role in intestinal inflammation. Peptides 2006; 27: 2434–2444.
12. Ramez M, Bagot M, Nikolova M, Boumsell L, Vita N, Chalon P, Caput D, Ferrara P, Bensussan A. Functional characterization of neurotensin receptors in human cutaneous T cell lymphoma malignant lymphocytes. J Invest Dermatol 2001; 117:687–693.
13. Vincent J-P, Mazella J, Kitabgi P. Neurotensin and neurotensin receptors. Trends Pharmacol Sci 1999; 20:302–309.
14. Pelaprat D. Interactions between neurotensin receptors and G proteins. Peptides 2006; 27:2476–2487.
15. Dupouy S, Mourra N, Doan VK, Gompel A, Alifano M, Forgez P. The potential use of the neurotensin high affinity receptor 1 as a biomarker for cancer progression and as a component of personalized medicine in selective cancers. Biochimie 2011; 93:1369–1378.
16. Miller LA, Cochrane DE, Carraway RE, Feldberg RS. Blockade of mast cell histamine secretion in response to neurotensin by SR 48692, a nonpeptide antagonist of the neurotensin brain receptor. Br J Pharmacol 1995; 114:1466–1470.
17. Yamauchi R, Wada E, Yamada D, Yoshikawa M, Wada K. Effect of beta-lactotensin on acute stress and fear memory. Peptides 2006; 27: 3176–3182.
18. Zhao D, Zhan Y, Zhan Y, Zeng H, Koon HW, Moyer MP, Pothoulakis C. Neurotensin stimulates expression of early growth response gene-1 and EGF receptor through MAP kinase activation in human colonic epithelial cells. Int J Cancer 2007; 120:1652–1656.
19. Antonelli T, Fuxe K, Tomasini MC, Mazzoni E, Agnati LF, Tanganelli S, Ferraro L. Neurotensin receptor mechanisms and its modulation of glutamate transmission in the brain: relevance for neurodegenerative diseases and their treatment. Prog Neurobiol 2007; 83:92–109.
20. Bian F, Mao G, Guo M, Mao G, Wang J, Li J, Han Y, Chen X, Zhang M, Xia G. Gradients of natriuretic peptide precursor A (NPPA) in oviduct and of natriuretic peptide receptor 1 (NPR1) in spermatozoon are involved in mouse sperm chemotaxis and fertilization. J Cell Physiol 2012; 227: 2230–2239.
21. Kumaresan A, Johannisson A, Humblot P, Bergqvist AS. Oviductal fluid modulates the dynamics of tyrosine phosphorylation in cryopreserved boar spermatozoa during capacitation. Mol Reprod Dev 2012; 79:525–540.
22. Baldi E, Luconi M, Muratori M, Marchiani S, Tamburrino L, Forti G. Nongenomic activation of spermatozoa by steroid hormones: facts and fictions. Mol Cell Endocrinol 2009; 308:39–46.
23. Quinn P, Kerin JF, Warnes GM. Improved pregnancy rate in human in vitro fertilization with the use of a medium based on the composition of human tubal fluid. Fertil Steril 1985; 44:493–498.
24. Fukami K, Yoshida M, Inoue T, Kurokawa M, Fissore RA, Yoshida N, Mikoshiba K, Takenawa T. Phospholipase Cdelta4 is required for Ca2+ mobilization essential for acrosome reaction in sperm. J Cell Biol 2003; 161:79–88.
25. Visconti PE, Bailey JL, Moore GD, Pan D, Olds-Clarke P, Kopf GS.

Capacitation of mouse spermatozoa. I. Correlation between the capacitation state and protein tyrosine phosphorylation.Development 1995; 121: 1129–1137.
26. Matsuyama S, Fukui R, Higashi H, Nishi A. Regulation of DARPP-32 Thr75 phosphorylation by neurotensin in neostriatal neurons: involvement of glutamate signalling. Eur J Neurosci 2003; 18:1247–1253.
27. Matsuyama S, Higashi H, Maeda H, Greengard P, Nishi A. Neurotensin regulates DARPP-32 thr34 phosphorylation in neostriatal neurons by activation of dopamine D1-type receptors. J Neurochem 2002; 81: 325–334.
28. Breitbart H. Signaling pathways in sperm capacitation and acrosome reaction. Cell Mol Biol (Noisy-Le-Grand) 2003; 49:321–327.
29. Mazella J, Zsurger N, Navarro V, Chabry J, Kaghad M, Caput D, Ferrara P, Vita N, Gully D, Maffrand JP, Vincent JP. The 100-kDa neurotensin receptor is gp95/sortilin, a non-G-protein-coupled receptor. J Biol Chem 1998; 273:26273–26276.
30. Nielsen MS, Jacobsen C, Olivecrona G, Gliemann J, Petersen CM. Sortilin/neurotensin receptor-3 binds and mediates degradation of lipoprotein lipase. J Biol Chem 1999; 274:8832–8836.
31. Navarro V, Martin S, Sarret P, Nielsen MS, Petersen CM, Vincent J, Mazella J. Pharmacological properties of the mouse neurotensin receptor 3. Maintenance of cell surface receptor during internalization of neurotensin. FEBS Lett 2001; 495:100–105.
32. Talbot P, Summers RG, Hylander BL, Keough EM, Franklin LE. The role of calcium in the acrosome reaction: an analysis using ionophore A23187. J Exp Zool 1976; 198:383–392.
33. Breitbart H. Intracellular calcium regulation in sperm capacitation and acrosomal reaction. Mol Cell Endocrinol 2002; 187:139–144.
34. Bourcier T, Rondeau N, Paquet S, Forgez P, Lombet A, Pouzaud F, Rostene W, Borderie V, Laroche L. Expression of neurotensin receptors in human corneal keratocytes. Invest Ophthalmol Vis Sci 2002; 43: 1765–1771.
35. Goedert M, Pinnock RD, Downes CP, Mantyh PW, Emson PC. Neurotensin stimulates inositol phospholipid hydrolysis in rat brain slices. Brain Res 1984; 323:193–197.
36. Chavarria ME, Reyes A. Secretions of ovine uterus and oviduct induce in vitro capacitation of ram spermatozoa. Arch Androl 1996; 36:17–23.
37. Parrish JJ, Susko-Parrish JL, Handrow RR, Sims MM, First NL. Capacitation of bovine spermatozoa by oviduct fluid. Biol Reprod 1989; 40:1020–1025.
38. Bathla H, Guraya SS, Sangha GK. Role of estradiol in the capacitation and acrosome reaction of hamster epididymal spermatozoa in the isolated uterus of mice incubated in vitro. Indian J Physiol Pharmacol 1999; 43: 211–217.
39. Mingoti GZ, Garcia JM, Rosa-e-Silva AA. Steroidogenesis in cumulus cells of bovine cumulus-oocyte-complexes matured in vitro with BSA and different concentrations of steroids. Anim Reprod Sci 2002; 69:175–186.
40. Oren-Benaroya R, Orvieto R, Gakamsky A, Pinchasov M, Eisenbach M. The sperm chemoattractant secreted from human cumulus cells is progesterone. Hum Reprod 2008; 23:2339–2345.
41. Park JY, Su YQ, Ariga M, Law E, Jin SL, Conti M. EGF-like growth factors as mediators of LH action in the ovulatory follicle. Science 2004; 303:682–684.
42. Su YQ, Nyegaard M, Overgaard MT, Qiao J, Giudice LC. Participation of mitogen-activated protein kinase in luteinizing hormone-induced differential regulation of steroidogenesis and steroidogenic gene expression in mural and cumulus granulosa cells of mouse preovulatory follicles. Biol Reprod 2006; 75:859–867.
43. Smith TT, Yanagimachi R. Attachment and release of spermatozoa from the caudal isthmus of the hamster oviduct. J Reprod Fertil 1991; 91: 567–573.
44. Su YQ, Wigglesworth K, Pendola FL, O'Brien MJ, Eppig JJ. Mitogen-activated protein kinase activity in cumulus cells is essential for gonadotropin-induced oocyte meiotic resumption and cumulus expansion in the mouse. Endocrinology 2002; 143:2221–2232.
45. Su YQ, Denegre JM, Wigglesworth K, Pendola FL, O'Brien MJ, Eppig JJ. Oocyte-dependent activation of mitogen-activated protein kinase (ERK1/2) in cumulus cells is required for the maturation of the mouse oocyte-cumulus cell complex. Dev Biol 2003; 263:126–138.
46. Zheng CF, Guan KL. Cytoplasmic localization of the mitogen-activated protein kinase activator MEK. J Biol Chem 1994; 269:19947–19952.
47. Li M, Liang CG, Xiong B, Xu BZ, Lin SL, Hou Y, Chen DY, Schatten H, Sun QY. PI3-kinase and mitogen-activated protein kinase in cumulus cells mediate EGF-induced meiotic resumption of porcine oocyte. Domest Anim Endocrinol 2008; 34:360–371.
48. Favata MF, Horiuchi KY, Manos EJ, Daulerio AJ, Stradley DA, Feeser WS, Van Dyk DE, Pitts WJ, Earl RA, Hobbs F, Copeland RA, Magolda RL, et al. Identification of a novel inhibitor of mitogen-activated protein kinase kinase. J Biol Chem 1998; 273:18623–18632.

FEBS Letters 588 (2014) 2003–2008

FEBS Letters

journal homepage: www.FEBSLetters.org

Site-specific phosphorylation of Tau protein is associated with deacetylation of microtubules in mouse spermatogenic cells during meiosis

Hiroki Inoue [a], Yuuki Hiradate [a], Yoshiki Shirakata [a], Kenta Kanai [b], Keita Kosaka [b], Aina Gotoh [b], Yasuhiro Fukuda [c], Yutaka Nakai [c], Takafumi Uchida [b], Eimei Sato [d], Kentaro Tanemura [a,*]

[a] Laboratory of Animal Reproduction and Development, Graduate School of Agricultural Science, Tohoku University, 1-1 Tsutsumidori-Amamiyamachi, Aobaku, Sendai 981-8555, Japan
[b] Molecular Enzymology, Department of Molecular Cell Science, Tohoku University, 1-1 Tsutsumidori-Amamiyamachi, Aobaku, Sendai 981-8555, Japan
[c] Laboratory of Sustainable Environmental Biology, Graduate School of Agricultural Science, Tohoku University, 232-3 Yomogida, Naruko-onsen, Osaki, Miyagi 989-6711, Japan
[d] National Livestock Breeding, 1 Odakurahara, Odakura, Nishigo-mura, Nishishirakawa-gun, Fukushima 961-8511, Japan

ARTICLE INFO

Article history:
Received 12 February 2014
Revised 26 March 2014
Accepted 10 April 2014
Available online 24 April 2014

Edited by Jesus Avila

Keywords:
Meiosis
Spermatogenesis
Testis
Tau

ABSTRACT

Tau is one of the microtubule-associated proteins and a major component of paired helical filaments, a hallmark of Alzheimer's disease. Its expression has also been indicated in the testis. However, its function and modification in the testis have not been established. Here, we analyzed the dynamics of phosphorylation patterns during spermatogenesis. The expression of Tau protein and its phosphorylation were shown in the mouse testis. Immunohistochemistry revealed that the phosphorylation was strongly detected during meiosis. Correspondingly, the expression of acetylated tubulin was inversely weakened during meiosis. These results suggest that phosphorylation of Tau protein contributes to spermatogenesis, especially in meiosis.

1. Introduction

The seminiferous epithelium of the mammalian testis possesses a variety of microtubule networks: an ordered array in Sertoli cells [1], the manchette, axonemal microtubules and in mitotic and meiotic spindles. These abundant microtubule networks are reflected by a diversity of microtubule-associated proteins (MAPs). Therefore, the testis can be a rich source for studies of microtubules and MAPs.

The tau (tubulin-associated unit) protein was identified in 1975 as a protein with the ability to induce microtubule formation [2,3]. Normally, tau is associated with microtubules and promotes their polymerization [3] and stabilization [4,5] depending on its phosphorylation status. For example, highly phosphorylated tau, which is observed in the brains of subjects with Alzheimer's disease (AD), composes paired helical filaments (PHFs) and barely promotes microtubule polymerization [6]. In the central nervous system, alternative splicing of the tau primary transcript generates six isoforms of 352–441 amino acids with an apparent molecular weight of 48–67 kDa [7–9]. Among the 85 putative phosphorylation sites on tau, 45 are serines, 35 are threonines and only 5 are tyrosines [10–12]. Tau is subdivided into four regions: an acidic region in the *N*-terminal part, a proline-rich region, a region responsible for binding with microtubules (microtubule-binding domains), and a C-terminal region. Serine phosphorylation at KXGS motifs, belonging to the microtubule-binding domain, decreases tau affinity for microtubules and consequently prevents binding to them [13–15]. Because more phosphorylated tau protein at Thr181, Ser199 and Thr231, belonging to the proline-rich region, is contained in the cerebrospinal fluid of brains from people with AD than in normal brains, it is useful as a biomarker of AD [16–18].

Although tau expression in the testis has been indicated [9,19], its expression and post-translational modification patterns including phosphorylation are barely known for this organ. In rat testis, tau was detected as two major bands with molecular masses of 34 and 37 kDa, and it has been suggested that tau is highly phosphorylated [9]. Phosphorylation, as mentioned above, is one of the most important post-translational modifications. To help elucidate the mechanisms of its function, we analyzed the dynamics of

* Corresponding author. Fax: +81 22 717 8686.
E-mail address: kentaro@m.tohoku.ac.jp (K. Tanemura).

http://dx.doi.org/10.1016/j.febslet.2014.04.021

tau protein expression and post-translational modification, especially phosphorylation, during mouse spermatogenesis.

2. Materials and methods

2.1. Animals

Male C57BL/6 mice at 12 weeks of age were used. All mice were anesthetized with 2, 2, 2-tribromoethanol and perfused with a physiological salt solution before being used for tissue collection. Care and use of the mice conformed to the Regulations for Animal Experiments and Related Activities at Tohoku University.

2.2. Antibodies

Several well-characterized antibodies to phosphorylated tau were used to investigate the level and phosphorylation states of tau protein in the testis. These antibody targets included mouse monoclonal antibody Ms X tau-1 [20] (#MAB3420, Lot: LV1478875, Chemicon), rabbit polyclonal antibody anti-phosphorylated tau^{S199,S202} (p-tau^{S199,S202}) [21] (#54963, Lot: HB131, AnaSpec) and mouse monoclonal antibodies, AT8 [22] (#MN1020, Lot: NG173165, Thermo Fisher Scientific), AT100 [23] (#MN1060, Lot: NE172687, Thermo Fisher Scientific), AT180 [24] (#MN1040, Lot: NJ176312, Thermo Fisher Scientific) and AT270 [25] (#MN1050, Lot: ND169027, Thermo Fisher Scientific). Anti-tau 1 recognizes the non-phosphorylated form of tau at Ser199 and Ser202. Anti-AT8 recognizes tau phosphorylation at Ser202 and Thr205. Therefore a mixture of anti-tau 1 and anti-AT8 is used for detection of total-tau. Anti-AT100 recognizes tau phosphorylation at Ser212 and Thr214. Anti-AT180 recognizes tau phosphorylation at Thr231. AT270 recognizes tau phosphorylation at Thr181. Anti-AT8, -AT100, -AT180 and -AT270 recognize PHF-tau. In addition, an anti-acetylated tubulin mouse monoclonal antibody [26] (#sc-23950, Lot: B0711, Santa Cruz), which indicates tubulin stabilization, was used. In Western blot analysis, a horseradish peroxidase conjugated second antibody (Promega; diluted 1:2000) was used. In immunohistochemistry, Alexa Flour 488-labeled anti-mouse secondary antibodies (Invitrogen; diluted 1:1000) were used against Tau1, AT8, AT100 and AT270. Alexa Fluor 488-labeled anti-rabbit secondary antibodies (Invitrogen; diluted 1:1000) were used against anti-p-tau^{S199,S202} antibodies. Alexa Fluor 568-labeled anti-mouse secondary antibodies (Invitrogen; diluted 1:1000) were used against anti-acetylated tubulin antibodies.

2.3. Molecular cloning of testis tau

Total RNA extraction from the testis was performed using an ISOGEN (Nippon Gene, Tokyo, Japan) and total RNA was stored at −80 °C until use. Poly (A) RNA was isolated using Poly (A) isolation Kit from Total RNA (Nippon Gene, Tokyo, Japan). Specific primers were designed on the basis of the sequences of Tau (forward: cag-gtcgaagattggctctact, reverse: ctggactctgtccttgaagtcc). The samples were reverse transcribed and cDNA synthesized using Rever Tra Ace (Nacalai Tesque). We acquired 286 bp partial sequence using taq DNA polymerase and following consensus primers obtained from mouse genes to initiate molecular cloning. For 3′RACE, PCR was performed using the gene specific primer 5′-gcc agg agg tgg cca ggt gga ag-3′ and specific adaptor primer (3′-Full RACE core Set, Takara, Kyoto Japan). For 5′RACE, PCR was performed using the gene specific primer, 5′-gct cag gtc cac cgg ctt gta gac-3′ and specific adaptor primer SMARTer RACE cDNA Amplification Kit (Takara, Kyoto, Japan). DNA sequencing was carried out with using the BigDye 3.1 reagent (Applied Biosystems, Tokyo, Japan) and 3130 genetic analyzer (Applied Biosystems, Tokyo, Japan).

2.4. Western blot analysis

Mouse testes ($n = 3$) were removed surgically and stored at −80 °C until use. Tris-Buffered Saline, protease inhibitor and phosphatase inhibitor were added to tissues then homogenized. Sample Buffer Solution with 2-mercaptoethanol (2×) for sodium dodecyl sulfate polyacrylamide gel electrophoresis (Nacalai Tesque, Kyoto, Japan) was added to the homogenized sample then sonicated. After boiling, samples were electrophoresed on polyacrylamide gels and transferred onto Immobilon-P transfer membranes (Millipore). These were incubated with Blocking One (Nacalai Tesque) then incubated with primary antibodies at 4 °C. Bound antibodies were detected by a horseradish peroxidase conjugated second antibody (Promega; diluted 1:2000) using an enhanced Chemi-Lumi One (Nacalai Tesque). Images were obtained with a Fujifilm LAS3000-mini image analysis system (Fujifilm Life Science, Tokyo, Japan) and analyzed with built-in software.

2.5. Immunohistochemistry

Mouse testes were removed surgically, fixed with methacarn (methanol:chloroform:acetic acid = 6:3:1) fixative, embedded in paraffin wax and sectioned. Cross-sections (10 μm) were deparaffinized then incubated with HistoVT One (Nacalai Tesque) at 90 °C for 30 min. After washing, sections were incubated with Blocking One (Nacalai Tesque) at 4 °C for 1 h then incubated with primary antibodies at 4 °C overnight. Immunoreactive elements were visualized with Alexa Fluor 488-labeled anti-rabbit secondary antibodies and Alexa Fluor 568-labeled anti-mouse secondary antibodies (Invitrogen; diluted 1:1000) by treating at 4 °C for 3 h. Nuclei were counterstained with Hoechst 33342 (Molecular Probes; diluted 1:5000). Stained images were obtained with an LSM-700 confocal laser microscope (Carl Zeiss, Oberkochen, Germany) and analyzed with ZEN-2010 software attached to the LSM-700.

3. Results

3.1. Determination of testis tau cDNA sequences

Analysis of tau cDNA sequence expressed in testis revealed that the sequence was confirmed with tau isoform-D (uniprot P10637-5)

3.2. Analysis of expression and phosphorylation pattern in the testis

In the testis, the anti-tau 1 antibody, which recognizes non-phosphorylation at Ser199 and Ser202, detected one major band with apparent molecular mass of 37 kDa and one minor band of 55 kDa in mice at 12 weeks of age (Fig. 1A). Anti-AT8, which recognizes phosphorylation at Ser202 and Thr205, detected several closely spaced bands with molecular masses between 50 and 60 kDa and two bands with apparent molecular mass of 40 and 37 kDa (Fig. 1B). Because detection of the antigen using tau 1 and AT8 antibody are almost complementary, immunohistochemistry using anti-tau 1 antibody and anti-AT8 antibody showed that total-tau protein was detected throughout spermatogenesis (Fig. 1C–E).

3.3. Dynamic changes in phosphorylation status

Immunohistochemistry using anti-AT8, -AT100 and -AT270 antibodies detected phosphorylated tau protein during spermatogenesis. Interestingly, spermatocytes during meiosis intensely stained with AT8, AT100 and AT270 (Fig. 2). AT8 and AT100 were localized all over spermatocytes except around the nucleus (asterisk in Fig. 2A and B). AT270 was detected in whole spermatocytes

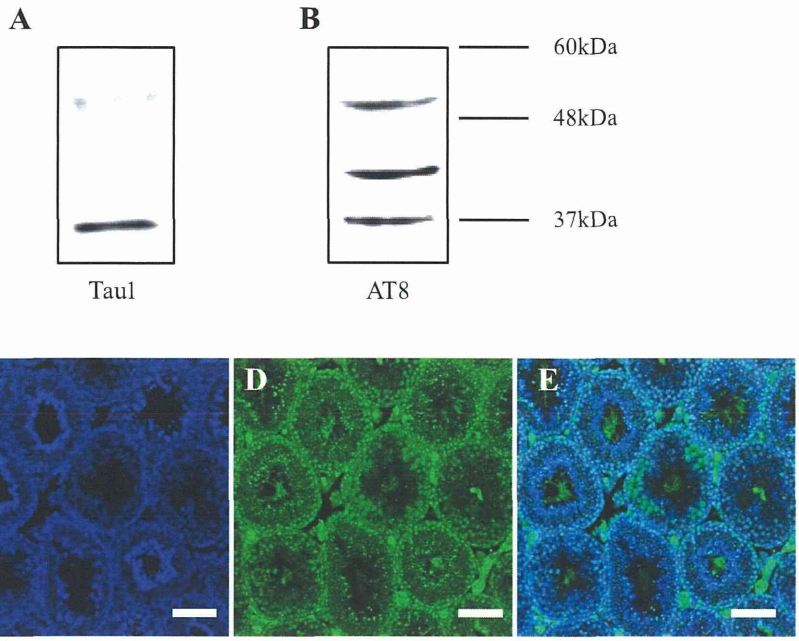

Fig. 1. Western blot analysis of testes from 12-week-old mice ($n = 3$). Tau protein was detected by antibodies against tau 1 (diluted 1:500) (A) and tau 5 (diluted 1:500) (B). Tau 1 detected one major band with molecular mass of 37 kDa and one minor band with molecular mass of 55 kDa (A). AT8 detected several closely spaced bands with molecular masses between 50 and 60 kDa, one major band with apparent molecular mass of 40 kDa and one minor band with apparent molecular mass of 37 kDa (B). Immunohistochemistry of the adult mouse testis. This section and the section in Fig. 3 are serial sections each other. Blue signals represent nuclear DNA counterstained with Hoechst 33342 (diluted 1:5000) (C). Green signals represent total-tau immunostained with anti-tau 1 (diluted 1:20) and anti-AT8 (diluted 1:20) (D). And merged image (E). Scale bar = 100 μm.

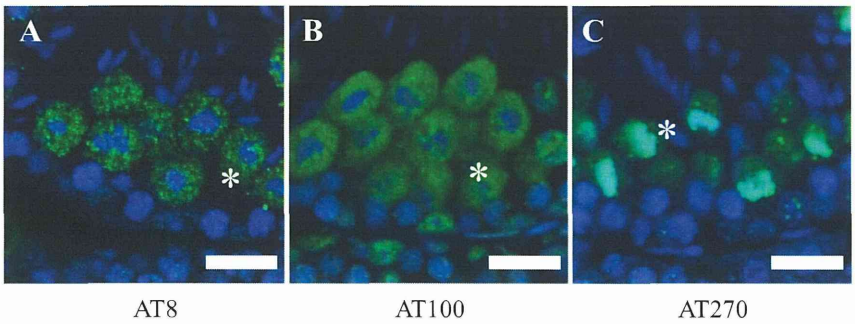

Fig. 2. Immunohistochemistry of the adult mouse testis. Images of seminiferous epithelia at stage XII. Zygotene spermatocytes, spermatocytes during meiotic division (indicated by asterisks) and step 12 elongating spermatids are present. Blue signals represent nuclear DNA counterstained with Hoechst 33342 (diluted 1:5000). Green signals represent immunostaining with anti-AT8 (diluted 1:50) (A), -AT100 (diluted 1:50) (B) and -AT270 (diluted 1:500) (C) antibodies. Scale bars = 20 μm.

and, in contrast to other antibodies, it was detected intensely at the nucleus (asterisk in Fig. 2C). P-tau^{T231} was not detected by anti-AT180 (data not shown).

In order to investigate the effect of tau phosphorylation on tubulin modification, we performed double staining with the anti-p-tau^{S199,S202} antibody and anti-acetylated tubulin antibody on serial sections. P-tau^{S199,S202} antibody detected phosphorylated tau protein during spermatogenesis. P-tau^{S199,S202} was also intensely stained in spermatocytes during meiosis (Fig. 3). Acetylated tubulin was almost not detected in spermatocytes during meiosis (Fig. 3). In order to investigate localization patterns of p-tau^{S199,S202} during spermatogenesis, we classified sections of seminiferous tubules under five stages, stage I, V, VIII, X and XII. Stage classification was based on Staging for Laboratory Mouse [27]. P-tau^{S199,S202} was detected from spermatogonia to step 8 round spermatids (Fig. 4). Spermatocytes during meiosis were intensely stained for p-tau^{S199,S202} (arrows in Fig. 4U–X). Conversely, staining with the anti-acetylated tubulin antibody showed that acetylated tubulin was expressed in spermatogenic cells from diplotene spermatocytes (arrowheads in Fig. 4Q–T) to step 8 round spermatids (asterisks in Fig. 4E–H), but was not detected in spermatocytes during meiosis (arrows in Fig. 4U–X). Double staining with the anti-p-tau^{S199,S202} antibody and anti-acetylated tubulin antibody revealed that the expression of acetylated tubulin decreased as p-tau^{S199,S202} increased. The latter was expressed all over spermatocytes except around the nucleus.

4. Discussion

Tau promotes tubulin assembly in vitro [3] and stabilizes microtubules against depolymerization in vivo [4,5]. An increase in tau phosphorylation reduces its affinity for microtubules, which results in neuronal cytoskeleton destabilization [28]. Conversely, the function of tau protein and its phosphorylation in the testis have not been characterized although its presence has been suggested [9,19].

Western blot analysis showed tau 1 and AT8 detect some bands with apparent molecular masses between 37 and 40 kDa in the

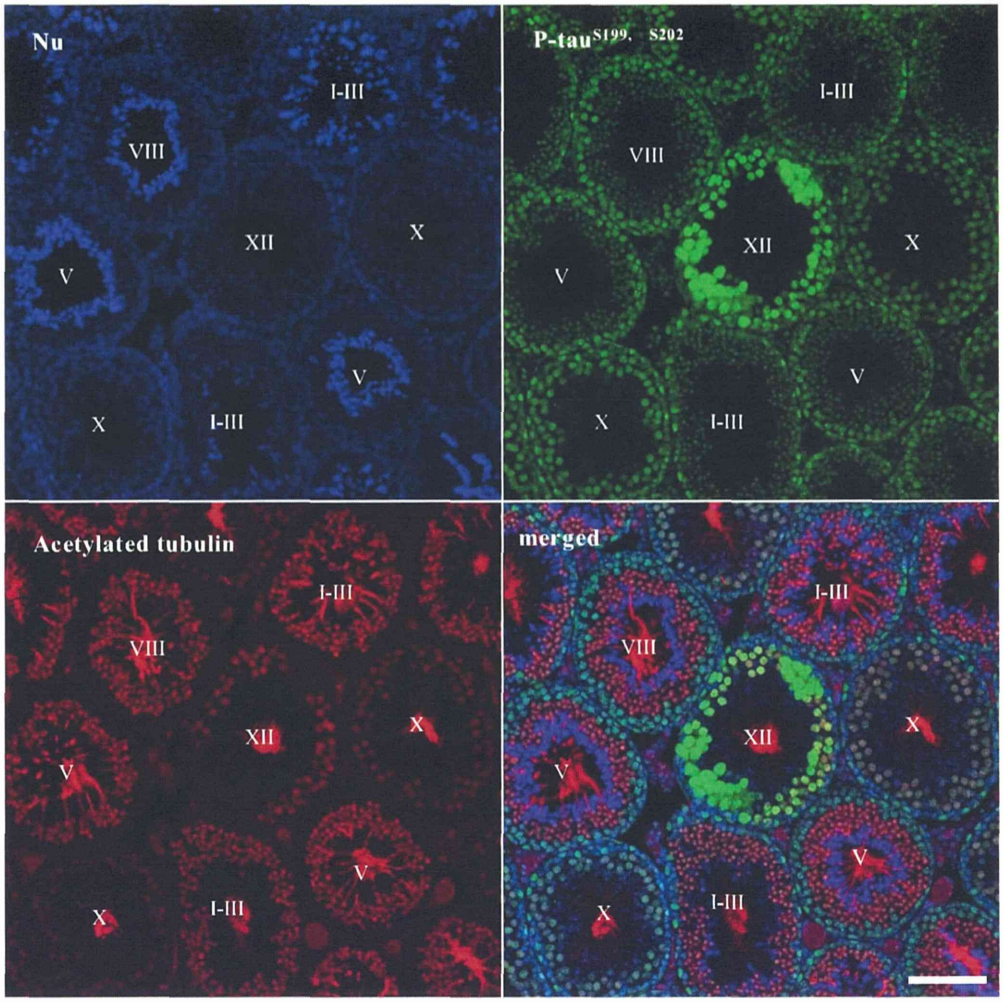

Fig. 3. Immunohistochemistry of adult mouse testis. Blue signals represent DNA counterstaining with Hoechst 33342 (diluted 1:5000). Green signals represent immunostaining for P-tau^{S199,S202} (diluted 1:1000). Red signals represent immunostaining for acetylated tubulin (diluted 1:500). Stages of seminiferous tubules were indicated. Scale bar = 100 μm.

mouse testis (Fig. 1A and B). To date, it has also been reported in the bull and rat [9,19]. In the adult rat brain, alternative splicing of the primary transcript of tau generates six isoforms with an apparent molecular weight between 48 and 67 kDa. However, Gu et al show tau protein was detected in two major bands in the testis with an apparent molecular mass of 34 and 37 kDa after alkaline phosphatase treatment. They suggest this different expression pattern indicates the presence of a testis-specific isoform [9]. In mouse, tau isoform-D (identifier: P10637-5) (uniprot) which molecular weight is about 39 kDa has been discovered [29]. Our sequencing of tau cDNA in the testes ensured that testis tau is corresponding with tau isoform-D. Our Western blot results also demonstrated that the presence of total tau protein with apparent molecular masses of 37 kDa in adult mice (Fig. 1A and B), consistent with previous reports. Furthermore, immunohistochemistry was performed to investigate the localization of phosphorylated tau.

PHFs are composed of highly phosphorylated tau and accumulate in the brain of subjects with AD [30,31]. To elucidate the localization of site-specific phosphorylation status, several antibodies against p-tau were used. The anti-AT8, -AT100 and -AT270 antibodies recognize PHF-tau. Immunohistochemical studies indicated not only tau expression but also its phosphorylation patterns in the testis. Although total-tau expression, detected by anti-tau 1 and anti-AT8 and non-phosphorylated tau at S199, S202, detected by anti-tau 1, were constantly observed from spermatogonia to round spermatids (Fig. 1C–E, S1), p-tau^{S199,S202}, AT8, AT100 and AT270 were especially localized in spermatocytes during meiosis (Fig. 2–4). These results suggested that tau expression was not specific during meiosis but the phosphorylation is specific. In addition, because these antibodies specifically detected the phosphorylation in meiosis, we suggest that Tau might be phosphorylated at AD-specific sites in meiosis. Interestingly, the period of tubulin deacetylation was coincident with that of tau phosphorylation at the time of meiosis (Fig. 4A–D, U–X). The relationship between tau phosphorylation and tubulin acetylation is unidentified. However, North and Verdin reported that activity of the microtubule deacetylase, SIRT2, was elevated during mitotic division, suggesting its involvement in destabilization of the spindle microtubule for chromosome movements [32]. On the other hand, tau acts as HDAC6 inhibitor and PHFs exert the stronger inhibiting actions than tau [33]. During spermatogenesis, the expression level of HDAC6 was high in spermatogonia and low from pachytene spermatocytes to elongating spermatids [34]. Therefore, these site-specific phosphorylation localizations suggest involvement of spindle microtubule destabilization during meiotic division. Further studies are necessary to clarify the relation between tau and microtubule deacetylases.

Chromosomal segregation in both mitotic and meiotic division is controlled by spindle microtubule elongation and retraction.

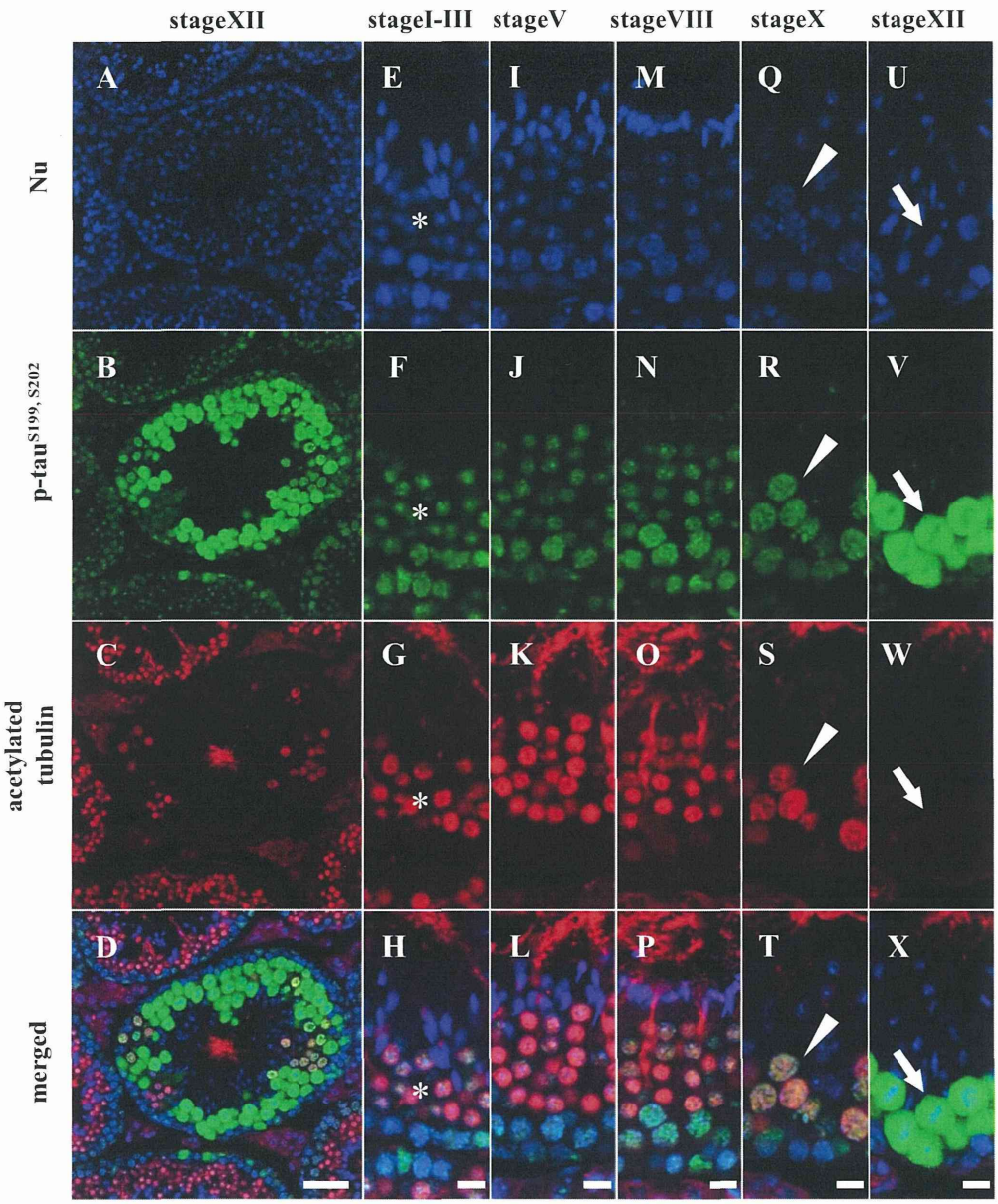

Fig. 4. Immunohistochemistry of adult mouse testis. (A, E, I, M, Q, U) Blue signals represent DNA counterstaining with Hoechst 33342 (diluted 1:5000). (B, F, J, N, R, V) Green signals represent immunostaining for P-tau^{S199,S202} (diluted 1:1000). (C, G, K, O, S, W) Red signals represent immunostaining for acetylated tubulin (diluted 1:500). (D, H, L, P, T, X) Merged Images. (A–D) Images of seminiferous tubules at stage XII. (E–X) Images of seminiferous epithelia. (E–H) Seminiferous epithelia at stages I–III. Early pachytene spermatocytes, step 1 round spermatids (asterisks) and step 13 elongated spermatids are present. (I–L) Seminiferous epithelium at stage V. Intermediate spermatogonia, pachytene spermatocytes, step 5 round spermatids and step 15 elongated spermatids are present. (M–P) Seminiferous epithelium at stage VIII. Preleptotene spermatocytes, pachytene spermatocytes, step 7 round spermatids and step 16 elongated spermatids are present. (Q–T) Seminiferous epithelium at stage X. Leptotene spermatocytes, late pachytene spermatocytes (indicated by arrowheads) and step 10 elongating spermatids are present. (U–X) Seminiferous epithelium at stage XII. Zygotene spermatocytes, spermatocytes during meiotic division (arrows) and step 12 elongating spermatids are present. (A–D) Scale bars in A–D = 50 μm; scale bars in E–X = 10 μm.

Segregation errors during meiotic division cause chromosomal aberrations, which if transferred to offspring cause malformation and miscarriage. Spindles, mainly composed of microtubules, are controlled by MAPs. It is known that spindle microtubules repeatedly extend and retract to catch the kinetochores of chromosomes during metaphase of mitotic and meiotic divisions [35,36]. Therefore, phosphorylation of the protein might contribute to this extension and retraction of microtubules during meiotic division.

Futhermore, the relationship between tau and DNA/chromosomes has recently reported. Tau has been reported to protect DNA from Oxidation and heat stresses [37,38]. In this study, P-tau^{S202,T205} and P-tau^{S212,T214} are localized all over spermatocytes except around the nucleus (Fig. 2A and B). This result agrees with the previous report [38]. In addition, P-tau^{T181} is localized at the nucleus (Fig. 2C). These results suggest that tau may interact with DNA/chromosomes also in the testis.

In conclusion, we have revealed that site-specific tau phosphorylation is localized specifically during spermatogenesis. Furthermore, there appears to be an interaction between tau phosphorylation and microtubule deacetylation, suggesting the possibility of involvement of both processes during meiosis.

Appendix A. Supplementary data

Supplementary data associated with this article can be found, in the online version, at http://dx.doi.org/10.1016/j.febslet.2014.04.021.

References

[1] Neely, M.D. and Boekelheide, K. (1988) Sertoli cell processes have axoplasmic features: an ordered microtubule distribution and an abundant high molecular weight microtubule-associated protein (cytoplasmic dynein). J. Cell Biol. 107, 1767–1776.

[2] Cleveland, D.W., Hwo, S.Y. and Kirschner, M.W. (1977) Physical and chemical properties of purified tau factor and the role of tau in microtubule assembly. J. Mol. Biol. 116, 227–247.

[3] Weingarten, M.D., Lockwood, A.H., Hwo, S.Y. and Kirschner, M.W. (1975) A protein factor essential for microtubule assembly. Proc. Natl. Acad. Sci. U.S.A. 72, 1858–1862.

[4] Drubin, D.G. and Kirschner, M.W. (1986) Tau protein function in living cells. J. Cell Biol. 103, 2739–2746.

[5] Kanai, Y., Takemura, R., Oshima, T., Mori, H., Ihara, Y., Yanagisawa, M., Masaki, T. and Hirokawa, N. (1989) Expression of multiple tau isoforms and microtubule bundle formation in fibroblasts transfected with a single tau cDNA. J. Cell Biol. 109, 1173–1184.

[6] Yoshida, H. and Ihara, Y. (1993) Tau in paired helical filaments is functionally distinct from fetal tau: assembly incompetence of paired helical filament-tau. J. Neurochem. 61, 1183–1186.

[7] Goedert, M., Spillantini, M.G., Jakes, R., Rutherford, D. and Crowther, R.A. (1989) Multiple isoforms of human microtubule-associated protein tau: sequences and localization in neurofibrillary tangles of Alzheimer's disease. Neuron 3, 519–526.

[8] Goedert, M., Spillantini, M.G., Potier, M.C., Ulrich, J. and Crowther, R.A. (1989) Cloning and sequencing of the cDNA encoding an isoform of microtubule-associated protein tau containing four tandem repeats: differential expression of tau protein mRNAs in human brain. EMBO J. 8, 393–399.

[9] Gu, Y., Oyama, F. and Ihara, Y. (1996) Tau is widely expressed in rat tissues. J. Neurochem. 67, 1235–1244.

[10] Buee, L., Bussiere, T., Buee-Scherrer, V., Delacourte, A. and Hof, P.R. (2000) Tau protein isoforms, phosphorylation and role in neurodegenerative disorders. Brain Res. Brain Res. Rev. 33, 95–130.

[11] Hanger, D.P., Betts, J.C., Loviny, T.L., Blackstock, W.P. and Anderton, B.H. (1998) New phosphorylation sites identified in hyperphosphorylated tau (paired helical filament-tau) from Alzheimer's disease brain using nanoelectrospray mass spectrometry. J. Neurochem. 71, 2465–2476.

[12] Sergeant, N. et al. (2008) Biochemistry of Tau in Alzheimer's disease and related neurological disorders. Expert Rev. Proteomics 5, 207–224.

[13] Dickey, C.A. et al. (2007) The high-affinity HSP90-CHIP complex recognizes and selectively degrades phosphorylated tau client proteins. J. Clin. Invest. 117, 648–658.

[14] Drewes, G., Trinczek, B., Illenberger, S., Biernat, J., Schmitt-Ulms, G., Meyer, H.E., Mandelkow, E.M. and Mandelkow, E. (1995) Microtubule-associated protein/microtubule affinity-regulating kinase (p110mark). A novel protein kinase that regulates tau-microtubule interactions and dynamic instability by phosphorylation at the Alzheimer-specific site serine 262. J. Biol. Chem. 270, 7679–7688.

[15] Sengupta, A., Kabat, J., Novak, M., Wu, Q., Grundke-Iqbal, I. and Iqbal, K. (1998) Phosphorylation of tau at both Thr 231 and Ser 262 is required for maximal inhibition of its binding to microtubules. Arch. Biochem. Biophys. 357, 299–309.

[16] Ishiguro, K. et al. (1999) Phosphorylated tau in human cerebrospinal fluid is a diagnostic marker for Alzheimer's disease. Neurosci. Lett. 270, 91–94.

[17] Itoh, N. et al. (2001) Large-scale, multicenter study of cerebrospinal fluid tau protein phosphorylated at serine 199 for the antemortem diagnosis of Alzheimer's disease. Ann. Neurol. 50, 150–156.

[18] Hampel, H. et al. (2004) Measurement of phosphorylated tau epitopes in the differential diagnosis of Alzheimer disease: a comparative cerebrospinal fluid study. Arch. Gen. Psychiatry 61, 95–102.

[19] Ashman, J.B., Hall, E.S., Eveleth, J. and Boekelheide, K. (1992) Tau, the neuronal heat-stable microtubule-associated protein, is also present in the cross-linked microtubule network of the testicular spermatid manchette. Biol. Reprod. 46, 120–129.

[20] Kishi, M., Pan, Y.A., Crump, J.G. and Sanes, J.R. (2005) Mammalian SAD kinases are required for neuronal polarization. Science 307, 929–932.

[21] Lee, D.C. et al. (2010) LPS-induced inflammation exacerbates phospho-tau pathology in rTg4510 mice. J. Neuroinflammation 7, 56.

[22] Goedert, M., Jakes, R., Crowther, R.A., Cohen, P., Vanmechelen, E., Vandermeeren, M. and Cras, P. (1994) Epitope mapping of monoclonal antibodies to the paired helical filaments of Alzheimer's disease: identification of phosphorylation sites in tau protein. Biochem. J. 301 (Pt 3), 871–877.

[23] Mailliot, C., Bussiere, T., Caillet-Boudin, M.L., Delacourte, A. and Buee, L. (1998) Alzheimer-specific epitope of AT100 in transfected cell lines with tau: toward an efficient cell model of tau abnormal phosphorylation. Neurosci. Lett. 255, 13–16.

[24] Ho, Y.S. et al. (2012) Endoplasmic reticulum stress induces tau pathology and forms a vicious cycle: implication in Alzheimer's disease pathogenesis. J. Alzheimers Dis. 28, 839–854.

[25] Brecht, W.J. et al. (2004) Neuron-specific apolipoprotein e4 proteolysis is associated with increased tau phosphorylation in brains of transgenic mice. J. Neurosci. 24, 2527–2534.

[26] Wilson, C.H. and Christie, A.E. (2010) Distribution of C-type allatostatin (C-AST)-like immunoreactivity in the central nervous system of the copepod *Calanus finmarchicus*. Gen. Comp. Endocrinol. 167, 252–260.

[27] Russell, L.D. et al. (1990) Histological and Histopathological Evaluation of the Testis, Cache River Press, Chapter 4 Staging for Laboratory Species, pp. 119–21.

[28] Grundke-Iqbal, I., Iqbal, K., Tung, Y.C., Quinlan, M., Wisniewski, H.M. and Binder, L.I. (1986) Abnormal phosphorylation of the microtubule-associated protein tau (tau) in Alzheimer cytoskeletal pathology. Proc. Natl. Acad. Sci. U.S.A. 83, 4913–4917.

[29] Kenner, L. et al. (1994) Expression of three- and four-repeat tau isoforms in mouse liver. Hepatology 20, 1086–1089.

[30] Lee, V.M., Balin, B.J., Otvos Jr., L. and Trojanowski, J.Q. (1991) A68: a major subunit of paired helical filaments and derivatized forms of normal Tau. Science 251, 675–678.

[31] Goedert, M. (1993) Tau protein and the neurofibrillary pathology of Alzheimer's disease. Trends Neurosci. 16, 460–465.

[32] North, B.J. and Verdin, E. (2007) Interphase nucleo-cytoplasmic shuttling and localization of SIRT2 during mitosis. PLoS ONE 2, e784.

[33] Perez, M. et al. (2009) Tau – an inhibitor of deacetylase HDAC6 function. J. Neurochem. 109, 1756–1766.

[34] Hazzouri, M., Pivot-Pajot, C., Faure, A.K., Usson, Y., Pelletier, R., Sele, B., Khochbin, S. and Rousseaux, S. (2000) Regulated hyperacetylation of core histones during mouse spermatogenesis: involvement of histone deacetylases. Eur. J. Cell Biol. 79, 950–960.

[35] Walczak, C.E. and Heald, R. (2008) Mechanisms of mitotic spindle assembly and function. Int. Rev. Cytol. 265, 111–158.

[36] Kitajima, T.S., Ohsugi, M. and Ellenberg, J. (2011) Complete kinetochore tracking reveals error-prone homologous chromosome biorientation in mammalian oocytes. Cell 146, 568–581.

[37] Wei, Y., Qu, M.H., Wang, X.S., Chen, L., Wang, D.L., Liu, Y., Hua, Q. and He, R.Q. (2008) Binding to the minor groove of the double-strand, tau protein prevents DNA from damage by peroxidation. PLoS ONE 3, e2600.

[38] Sultan, A. et al. (2011) Nuclear tau, a key player in neuronal DNA protection. J. Biol. Chem. 286, 4566–4575.

Reproduction in Domestic Animals

Reprod Dom Anim 49. e26–e30 (2014); doi: 10.1111/rda.12289
ISSN 0936-6768

Short Communication

Hanging Drop Monoculture for Selection of Optimal Antioxidants During *In Vitro* Maturation of Porcine Oocytes

S Ishikawa[1], R Machida[1], K Hiraga[1], Y Hiradate[1], Y Suda[2] and K Tanemura[1]

[1]*Laboratory of Animal Reproduction and Development, Graduate School of Agricultural Science, Tohoku University, Sendai, Japan;* [2]*Department of Farm Management, School of Food, Agricultural and Environmental Sciences, Miyagi University, Sendai, Japan*

Contents

We analysed the effect of three antioxidants that have different functional mechanisms on the *in vitro* maturation (IVM) of porcine oocytes. Single oocyte monoculture using the hanging drop (HD) system has some advantages such as improving analysis efficiency brought by the smaller number of samples than the number of oocytes cultured in one drop. Direct effects of ligands on single oocytes could also be detected without considering the effects of paracrine factors from other oocytes. After 22 h of pre-culture, denuded oocytes were cultured for 22 h with 0.01 and 0.1 μg/ml of L-carnitine (LC), lactoferrin (LF) or sulforaphane (SF) in the presence/non-presence of oxidant stress induced by H_2O_2 supplementation to evaluate the reducing effects against oxidative stress on nuclear maturation. As a result, compared with LC and SF, LF showed effective reduction in oxidative stress at a lower concentration (0.01 μg/ml), suggesting that LF is a more effective antioxidant in porcine oocyte IVM. Additionally, LF also increased maturation rate even in culture without H_2O_2. Our results clearly suggest that the HD monoculture system is useful for screening the substances that affect porcine oocyte culture.

Introduction

During *in vitro* production (IVP) of porcine embryos, the immature ovum obtained from the ovary is matured *in vitro*. The likelihood that a blastocyst develops from a fertilised egg following *in vitro* fertilisation (IVF) is approximately 30–40% (Yoshioka et al. 2003; Suzuki et al. 2005), and the development of offspring by subsequent transplantation of IVP embryos is also low. It has been suggested that one factor contributing to low success rates is the accumulation of oxidative stress by reactive oxygen species (ROS) that arise from mitochondria in the oocytes. ROS are generated from oxygen molecules by some reductive reactions, broadly classified into two groups: radicals and non-radicals. To date, the hydroxyl radical (OH), peroxy radical (LOO) and hydroperoxy radical (HOO) have been classed in the radical group and hydrogen peroxide (H_2O_2) and lipid hydroperoxide (LOOH) in the non-radical group (Tatemoto et al. 2000; Guerin et al. 2001; Kitagawa et al. 2004; Kang et al. 2009). H_2O_2 generates OH and has high toxicity (Agarwal 2004). Furthermore, H_2O_2 generates lipid peroxide (LPO) that causes serious oxidative stress by targeting the lipid (Gutteridge 1994; Takahashi et al. 2003).

The huge amount of lipid in a porcine oocyte, compared with oocytes from other mammalian species, is mostly made up of triglycerides (TGs) (McEvoy et al. 2000; Sturmey and Leese 2003; Sturmey et al. 2009). TG plays an important role in energy metabolism by providing adenosine triphosphate (ATP) for protein synthesis, meiosis and cytoplasmic maturation (Sturmey and Leese 2003). In addition, it is recognised that TG is oxidised to LPO by H_2O_2 (Gutteridge 1994; Takahashi et al. 2003). In other words, it is thought to be susceptible to oxidative stress because porcine oocytes contain plenty of TG and is a target of LPO. Therefore, it is possible that one approach for improving the quality of oocytes matured *in vitro* is the addition of antioxidants to IVM medium, this actually has been performed in many species, and the selection of an effective antioxidant is important.

Here, we employed single oocyte monoculture using the hanging drop (HD) system, and it has been proven in the culture of other cells (Tung et al. 2010). The application of this culture method in IVM has some merits. One is the high-throughput efficiency of the experiment compared with conventional methods such as the culture drop (CD) method (Tung et al. 2010). The HD system is performed using a single oocyte per drop; hence, a number of conditions affecting individual oocytes can be evaluated at once.

Using the HD system, we selected three antioxidants to study: LC, LF and SF. Wu et al. (2011) reported that LC improves the nuclear maturation of porcine oocytes by reducing H_2O_2 levels in the oocytes. However, the effect of LF and SF on IVM of porcine oocytes has not been reported.

L-carnitine has a strong antioxidant power and scavenges H_2O_2 (Wu et al. 2011). Furthermore, it plays an important role in carrying free fatty acids essential for β-oxidation in mitochondria to the inner membrane (Hashimoto 2009). LF removes excessive free iron ions *in vivo* and inhibits the production of OH by chelate reactions (Gutteridge et al. 1981). Moreover, LF is thought to act on lipid metabolism by reducing the gene expression of perilipin that hinders the effect of lipase when TG is decomposed into fatty acid by lipase (Ono et al. 2011). SF is thought to act on deoxidisation of H_2O_2 and reduction in oxidative damage because it induces the production of phase 2 antioxidant enzymes (i.e. GST), and phase 2 antioxidant enzymes induce the production of glutathione (Fahey and Talalay 1999).

Here, the aim was to assess the effects of these antioxidants, which have different mechanisms on the